Geophysical Research Letters

RESEARCH LETTER
10.1029/2021GL095232

On Recent Large Antarctic Ozone Holes and Ozone Recovery Metrics

K. A. Stone[1], S. Solomon[1], D. E. Kinnison[2], and Michael J. Mills[2]

[1]Department of Earth, Atmospheric, and Planetary Science, Massachusetts Institute of Technology, Cambridge, MA, USA, [2]National Center for Atmospheric Research, Atmospheric Chemistry Observations and Modeling Laboratory, Boulder, CO, USA

Key Points:

- The seasonal onset of ozone depletion continues to slow down due to decreasing stratospheric chlorine and bromine concentrations
- Recent large ozone holes of 2015, 2018, 2020, and 2021 display slower seasonal onset compared to 1999–2008 despite record sizes later
- September ozone hole size trends over 2000–2021 at different depth thresholds (such as 220, 175, 130 DU) indicate recovery

Supporting Information:

Supporting Information may be found in the online version of this article.

Correspondence to:

K. A. Stone,
stonek@mit.edu

Citation:

Stone, K. A., Solomon, S., Kinnison, D. E., & Mills, M. J. (2021). On recent large Antarctic ozone holes and ozone recovery metrics. *Geophysical Research Letters*, *48*, e2021GL095232. https://doi.org/10.1029/2021GL095232

Received 14 JUL 2021
Accepted 7 NOV 2021

Abstract The 2015 and 2020 ozone holes set record sizes in October–December. We show that these years, as well as other recent large ozone holes, still adhere to a fundamental recovery metric: the later onset of early spring ozone depletion as chlorine and bromine diminishes. This behavior is also captured in the Whole Atmosphere Chemistry Climate Model. We quantify observed recovery trends of the onset of the ozone hole and in the size of the September ozone hole, with good model agreement. A substantial reduction in ozone hole depth during September over the past decade is also seen. Our results indicate that, due to dynamical phenomena, it is likely that large ozone holes will continue to occur intermittently in October–December, but ozone recovery will still be detectable through the later onset, smaller, and less deep September ozone holes: metrics that are governed more by chemical processes.

Plain Language Summary The ozone hole that forms every spring in the Southern Hemisphere over Antarctica is expected to recover within the next 50 years. However, there have been several large ozone holes recently. In 2015, a record large volcanic eruption injected a large amount of sulfur into the upper atmosphere, which helps deplete ozone. In 2020, the Australian bushfires also injected a large amount of aerosol into the upper atmosphere, with a possible similar consequence. In this study, we show that by investigating a key time period in the early spring when the ozone hole is forming, the dynamical influence and the influence of volcanic and bushfire aerosols on ozone depletion over Antarctica is not as important and therefore ozone recovery can still be detected.

1. Introduction

Antarctic ozone recovery is expected to continue in the 21st century, with October total column ozone (TCO) return dates to 1980 levels projected by 2060 (Dhomse et al., 2018). Significant detection of increasing ozone is therefore important for confirming that the recovery is proceeding as expected, and for verifying the success of the Montreal Protocal and subsequent amendments. This is especially significant due to the recent and unexpected increase in CFC-11 levels (Lickley et al., 2020; Montzka et al., 2018).

In the upper stratosphere mid and polar latitudes, ozone recovery from gas phase chemistry is expected to be detectable due to limited interannual variability, however, in the lower stratosphere polar regions, where heterogenous chemistry is greatest, variability is large, hindering the significance of recovery trends (e.g., Ivy et al., 2016; Stone et al., 2018; Weatherhead et al., 2000). There have been many recent studies that focus on the detectability of Antartic ozone recovery, especially during September (Kramarova et al., 2019; Pazmiño et al., 2018; Solomon et al., 2016; Strahan et al., 2014, 2019). September is the key time period because it is relatively stable dynamically and encompasses the initial onset and growth of ozone depletion when the sun emerges (e.g., Hassler et al., 2011). The photolysis of Cl_2 allows for the key ClO dimer and BrO–ClO catalytic cycles to occur (Molina et al., 1987; Solomon, 1999). Therefore, the rate of early-season ozone depletion is especially dependent on ClO concentrations, which in turn are related closely to equivalent effective stratospheric chlorine (EESC) (Engel et al., 2018; Newman et al., 2007). Dynamical variability coupled with saturation of ozone loss as concentrations are close to zero impede detection of recovery later in the season.

Indeed, Solomon et al. (2016) showed through the use of a chemistry climate model that Antarctic ozone depletion during September has begun to recover. Additionally, Kuttippurath et al. (2018) showed a reduced frequency of ozone loss saturation between 13 and 21 km. However, detecting recovery in observations can be hampered by a combination of large variability and limited years over the recovery period, that is, since

2000 (Chipperfield et al., 2017). An important recent paper by Pazmiño et al. (2018) reported significant ozone recovery through a reduction of the areas displaying exceptionally deep loss (e.g., under 175 Dobson Units [DU]) in recent years. Indicators of ozone recovery, such as minimum polar cap mean TCO and stratospheric partial columns, among others, were also reported in Bodeker and Kremser (2021).

In recent years, four large (i.e., spatially extensive but not necessarily deep) Antarctic ozone holes have occurred. In 2015, volcanic aerosols from the Calbuco volcanic eruption exacerbated ozone depletion, producing a record-large October ozone hole that lasted late in the season (Ivy et al., 2017; Solomon et al., 2016; Stone et al., 2017; Zhu et al., 2018). In 2020, the 2015 record was exceeded by an even larger and longer-lasting Antarctic ozone hole. There is evidence that large aerosol loading from the 2020 Australian bushfires may have intensified this depletion, similar to volcanic aerosols in 2015 (Yu et al., 2021). A large ozone hole also occurred in 2018 due solely to dynamical variability, which is also a major driver of ozone depletion; 2021 is also displaying a large ozone hole. Therefore, it is important to establish if recent years are calling the expected ozone recovery into question.

In this paper, we identify recovery metrics that are insensitive to the recent large ozone holes. These are: (a) the size of the ozone hole below 220 DU in September (size metric based on the standard threshold), (b) depth using lower total column thresholds for September, and (c) the ozone hole start dates. All three of these metrics are linked to the initial seasonal period of rapid ozone loss and reveal related behavior.

2. Observations and Model Data

We use observational data from the Bodeker Scientific Filled Total Column Ozone Database V3.5.2 (BS-TCO) (Bodeker, Kremser, & Tradowsky, 2021). This database combines TCO data from multiple different satellite-based instruments at a resolution of 1.25° longitude by 1° latitude and spanning the period of October 31, 1978 to December 31, 2019. Bodeker, Kremser, & Tradowsky, 2021 and Bodeker, Nitzbon, et al. (2021) use a machine learning approach to account for missing data, which is especially important for this paper as we make use of the polar regions. See Bodeker, Nitzbon, et al. (2021) for more information.

As BS-TCO data is not yet available for 2020 and 2021, we use Ozone Monitoring Instrument (OMI) satellite data. The instrument is an ultraviolet/visible nadir-viewing solar backscatter spectrometer and the data product is released as globally gridded observations at 1° latitude by 1° longitude (Levelt et al., 2006).

We use a 10 member ensemble of the Community Earth System Model, Version 1 (CESM1) Whole Atmosphere Chemistry Climate Model, Version 4 (WACCM4). This is a fully coupled chemistry climate model and has a horizontal resolution of 1.9° latitude by 2.5° longitude and 66 vertical levels with a high top at 5.1×10^{-6} hPa. The chemical scheme is the Model of Ozone and Related Tracers (Kinnison et al., 2007). We utilize a 10 member ensemble that is run over 1995–2024. Surface area densities (SAD) are prescribed from WACCM simulations including interactive stratospheric aerosol, and an emissions database over 1995–2014 (see Mills et al., 2016; Neely & Schmidt, 2016), after which a repeating 2000 year is used as it represents a background state without major volcanic aerosol. Therefore, Calbuco is not represented in this model. This version of WACCM4 has a prescribed repeating Quasi-Bienial Oscillation (QBO). See Stone et al. (2019) for more information.

In addition to WACCM4, we use data from a three-member ensemble of the newer model version CESM2 WACCM6 over 1980–2024. Over 1980–2014, the historical simulation is used. Over 2015–2024, the future projection simulations used follow SSP2-4.5 (Meinshausen et al., 2020), including constant SO_2 emissions representing the time average of all volcanic eruptions from 1850 to 2014. The model has a horizontal resolution of ~0.95° latitude by 1.25° longitude and 70 vertical levels with a high top at 4.5×10^{-6} hPa. It includes many advancements compared to WACCM4, notably, an interactive QBO and additions to the chemical schemes. See Gettelman et al. (2019) for more details.

3. Methods

The ozone hole size is calculated by summing all grid boxes south of 40°S where TCO is below a given threshold. Three different DU thresholds are used: 220 DU, 175 DU, and 130 DU. To test the hypothesis of later onset of ozone depletion in the model and to compare to the observed large ozone hole years, 6 model ensemble years for WACCM6 and 10 model ensemble years for WACCM4 between 2015 and 2020 that had the largest October ozone hole areas were extracted and averaged.

Missing OMI polar data for 2020 and 2021, when BS-TCO data are not available, are filled in. This is achieved by examining whether the southernmost datapoint available for a given longitude grid point is below the DU threshold, then assuming that missing data southwards are also below the threshold.

The start date of the ozone hole was calculated by finding the first date when the size of the ozone hole went above a selected size threshold and remained above for at least 3 days (to ensure persistence). The thresholds are: 8, 5, and 1 million km^2 for 220, 175, and 130 DU, respectively, based on behavior at the peak of EESC loading around the year 2000 (for 220 DU, 12, 10, and 8 million km^2 thresholds were investigated, with 8 million km^2 producing the strongest trends, see Figure S2).

Trends were calculated using a simple linear regression model. Representation of dynamical variability (such as the QBO) through a multiple linear regression was excluded here for simplicity. Therefore, trend values should not be taken as an optimal estimate. Trend significance is calculated by the 95th percentile following an F-test. Variability of the model ensemble is shown by plotting the ensemble standard deviation (SD).

4. Results

Figure 1 shows the ozone hole size over the course of August–December for BS-TCO, WACCM6, and WACCM4 for different time periods of ozone depletion and recovery, generally defined as: 1980–1988, the beginning of ozone depletion; 1999–2008, the peak of ozone depletion; 2009–2018, the beginning of ozone recovery, and 2019–2024; the model extended years.

For the 220 DU threshold (Figures 1a–1c), on average, observed ozone depletion typically begins at the start of August, peaks at the end of September and subsides by the end of the year. Periods with larger EESC loading and therefore large ozone depletion, such as 1999–2008, display an earlier sharp rise in ozone depletion and earlier peak in ozone hole area compared to other time periods. Both model ensemble means show qualitatively similar behavior in these characteristics. In contrast, during October and November, there is little change in the size of the observed ozone hole when comparing 1999–2008 to 2009–2018 in observations. This is also seen in WACCM6 in November. In WACCM4, the ozone hole opens slightly later and persists longer into the season, contrary to what was seen in the observations (also, see Figure S1). Earlier versions of WACCM did have a SH pole cold bias, but was mostly corrected in WACCM4 onwards through modification of the gravity wave scheme (Garcia et al., 2017). However, it is noteworthy that the closing of the hole can be expected to be dynamically dominated, while its formation is chemically dominated.

The large ozone holes of 2015, caused by Calbuco volcanic aerosols (Ivy et al., 2017; Solomon et al., 2016; Stone et al., 2017); 2018; 2020, likely exacerbated by the 2020 Australian bushfires (Yu et al., 2021); and 2021 are also plotted in Figures 1a, 1d, and 1e (shown in brown, orange, purple, and white, respectively). The size and persistence of the ozone holes during 2015 and 2020 are unusual, and combined, set records for size on almost all days after the second week of October (Figure 1a). The ozone hole in 2018 was also large, but did not set any records; 2021 was similar (up to October 31). Even though 2015, 2018, 2020, and 2021 had large ozone holes, there is a clear later onset of ozone depletion in these years compared to 1999–2008 (the peak in stratospheric EESC loading) expressing that ozone recovery is still proceeding following the decline in polar EESC since ~2000 (WMO, World Meteorological Organization, 2018). The 6 largest WACCM6 and 10 largest WACCM4 October ozone holes between 2015 and 2020 were averaged and plotted. For the 220 DU threshold, we see larger than average ozone holes during October compared to 1999–2008, but only a slight difference in the timing of the onset of depletion in WACCM6 and not much difference in WACCM4. However, for 175 and 130 DU, we do see a later start date in the onset of ozone depletion for both WACCM6 and WACCM4. We note that the rate of the key reactions of Antarctic ozone depletion, the ClO dimer

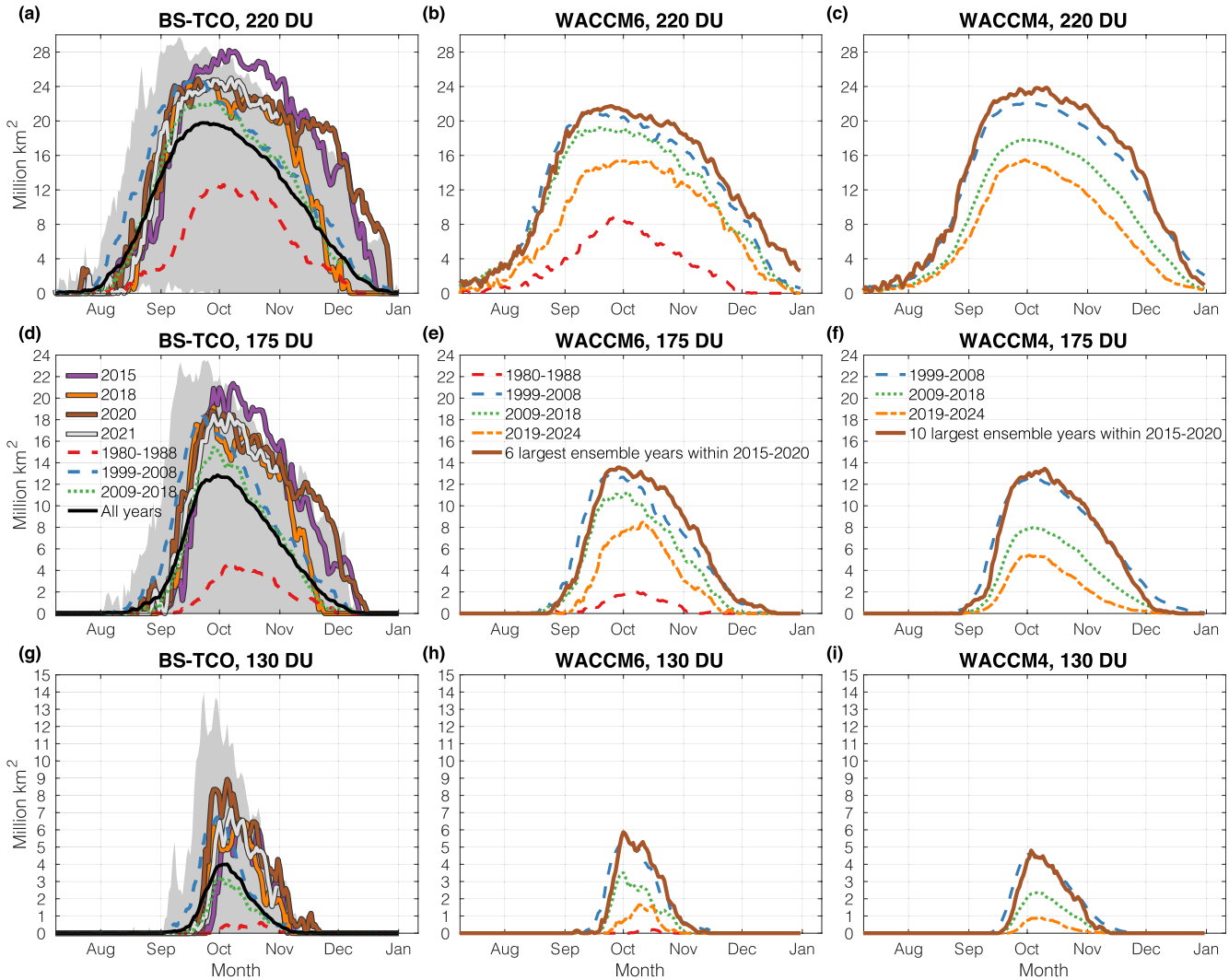

Figure 1. Daily ozone hole sizes over different mean time periods and different DU thresholds for Bodeker Scientific Filled Total Column Ozone (BS-TCO) (left panels), Whole Atmosphere Chemistry Climate Model, Version 6 (WACCM6) (middle panels), and WACCM4 (right panels). Overplotted on the observations are the four recent large ozone hole years of 2015, 2018, 2020, and 2021. The shaded region shows the total range of values excluding these years. The mean of the 6 and 10 largest ensemble years within the 2015–2020 range are overplotted on the WACCM6 and WACCM4 data, respectively.

and BrO-ClO catalytic cycles, are dependent on ClO concentrations (Molina et al., 1987; Solomon, 1999). Therefore, the initial rate of depletion is slower in 2015, 2018, 2020, and 2021 compared to 1999–2008 due to lower EESC concentrations.

Figure 2 shows time series of the ozone hole start date for both observations and the WACCM6 ensemble. This ensemble shows the best agreement with the observations in Figure 1 (comparison to the WACCM4 ensemble can be found in Figure S3). The threshold values, although arbitrary, capture ozone depletion and recovery trends in both the observations and the model. When using the 220 DU threshold (panel a), over the ozone depletion period (1979–1999), the ozone hole opens earlier every year with a statistically significant trend at the 95th percentile of -24.7 ± 6.5 days/decade. From 2000 onwards, a significant recovery trend in the start date of 8.1 ± 3.6 days/decade is seen. The observed recovery trends are broadly similar, but slightly less than, the WACCM6 ensemble. The 2015, 2018, 2020, and 2021 start dates are also not significant outliers in the observations.

When looking at the 175 DU threshold, which represents an example of a "deeper" portion of the ozone hole, the observed decreasing trend is not as large compared to the 220 DU threshold, at -18.0 ± 7.0 days/decade.

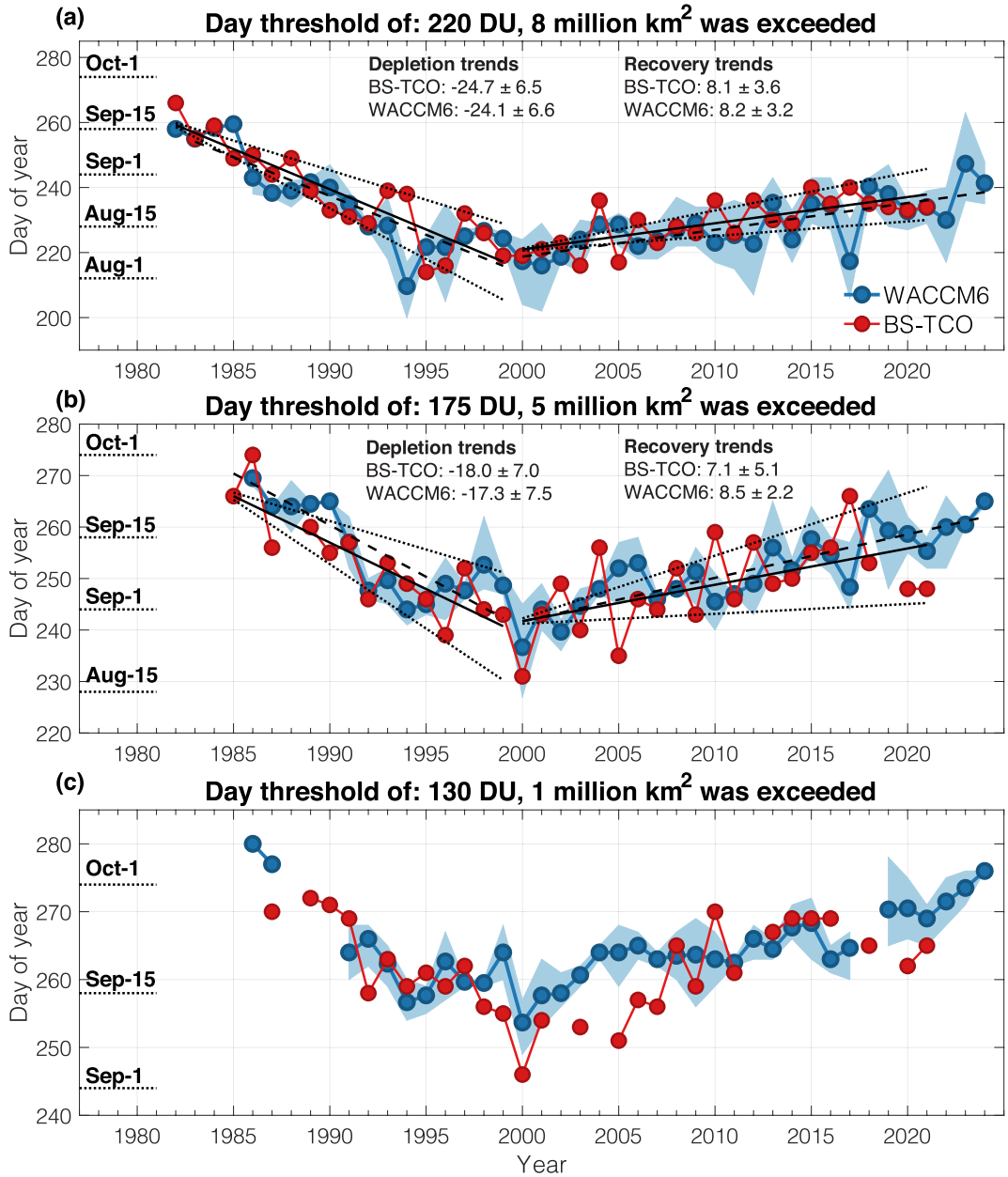

Figure 2. Observed and model ensemble ozone hole start dates for when the ozone hole exceeded the size thresholds of 8 million km^2 for 220 DU (a), 5 million km^2 for 175 DU (b), and 1 million km^2 for 130 DU (c). Trends as days/decade are shown over the depletion era at the first year of occurance to 1999 for observations and the model ensemble (solid and dashed lines, respectively), and for the recovery era of 2000–2021 in observations and 2000–2024 in the model ensemble. Trend 95th percent confidence intervals are shown for the observed trend lines in panels (a) and (b) (dotted lines). Model ensemble variability is shown as the shaded area for ±1 SD.

The recovery trend is, however, similar compared to the 220 DU threshold with a trend of 7.1 ± 5.1 days/decade. Interestingly, in 2019, we do not see the formation of an ozone hole at all for the first time since 1988 at 175 DU due to a sudden stratospheric warming that interrupted ozone loss (e.g., Yamazaki et al., 2020). The WACCM6 ensemble also shows a similar recovery trend magnitude for both the 220 and 175 DU thresholds.

The third threshold of deep depletion at 130 DU is interesting in that these values occurred in every year between 1987 (the first year) and 2001 (except for 1988) in the depletion time period, but are much rarer in the recovery period. This is also seen in the model ensemble, where in the last 5 years of 2000–2024,

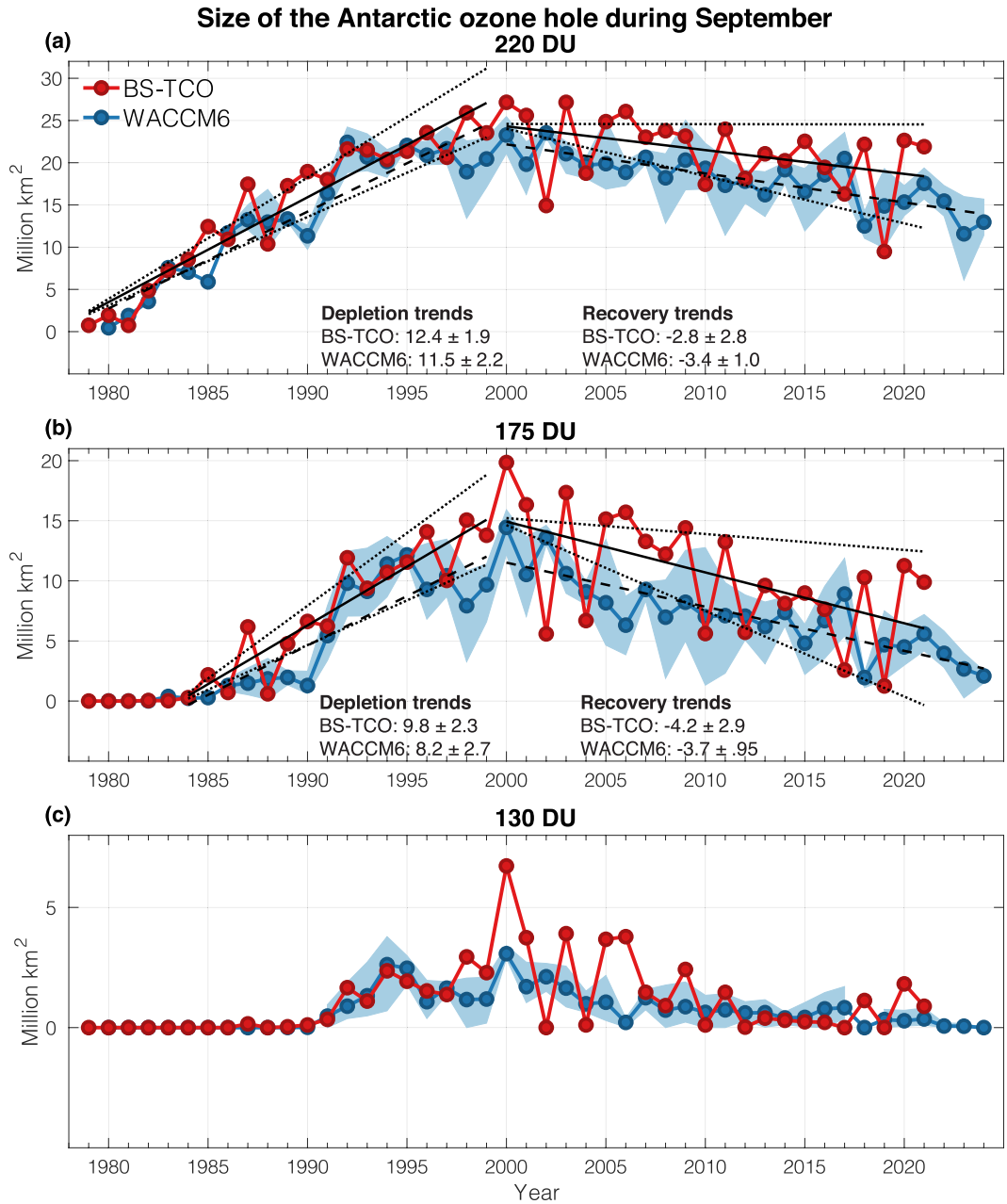

Figure 3. Same as Figure 2, but for the size of the September average ozone hole areas below 220 DU (a), 175 DU (b), and 130 DU (c). Observed and modeled depletion and recovery era trends are shown in million km^2/decade in (a) and (b).

only 60% of model years reached this threshold. Therefore, we can expect that very deep ozone holes will become exceedingly rare in the near future, as suggested in Pazmiño et al. (2018). Since a large number of years did not reach the threshold in the recovery era at all, trends were not calculated for 130 DU (similarly for Figures 3c and 4c).

A key take away from Figure 2, is that even though 2020 and 2015 had record large ozone holes later in the season, the ozone hole start dates occurred later than a majority of the years within the 1999–2008 decade. Only 2004 has a later start date than 2015, 2018, 2020, and 2021 for the 220 DU, 8 million km^2 threshold. For the deeper thresholds, 2002 and 2008 also have later start dates than 2020 and 2021, but not 2015 and 2018. Similar results are seen when using other size thresholds of 12 and 10 million km^2 for 220 DU (Figure S2).

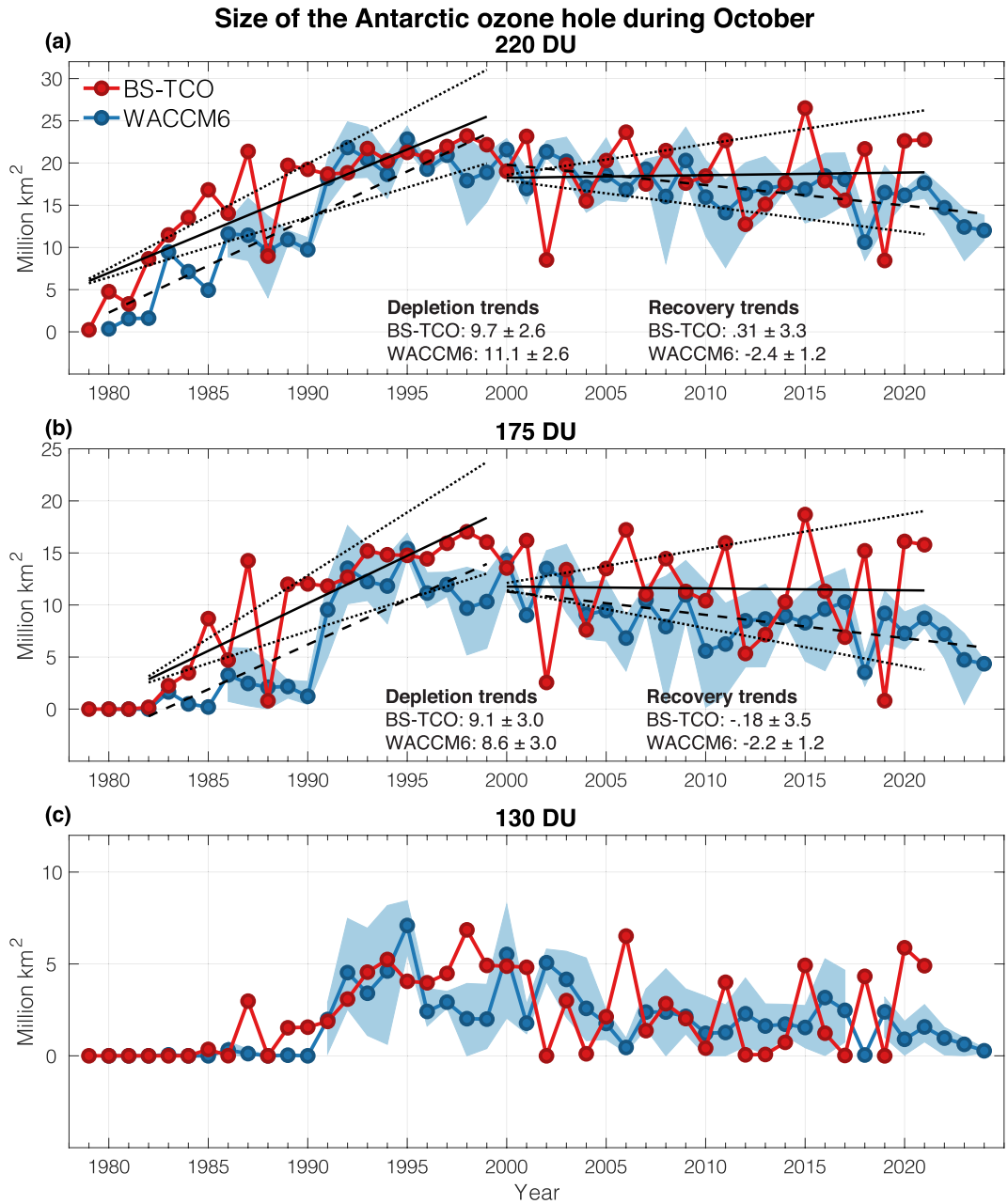

Figure 4. Same as Figure 3, but for October.

We next look at trends in the size of the ozone hole for September (Figure 3), a key time period to investigate ozone recovery, and compare to October (Figure 4). This is analyzed for the same thresholds of 220, 175, and 130 DU. During September for the 220 DU threshold, we see a clear and rapid increase in the size of the ozone hole over 1979–1999 at a rate of 12.4 ± 1.9 million km^2/decade. We then see a decreasing trend at around a quarter of the rate of the past trend of −2.8 ± 2.8 million km^2/decade. The rates of the trends are in good agreement with the model ensemble.

When we look at the deeper ozone hole threshold of 175 DU, the observed decreasing trend of −4.2 ± 2.9 million km^2/decade from 2000 to 2020 is larger, and more significant, than the 220 DU threshold. This is also seen in WACCM6, which has a slightly larger trend of −3.7 ± 0.95 million km^2/decade at 175 DU compared to −3.4 ± 1.0 million km^2/decade for 220 DU. However, this is not captured in the WACCM4 ensemble (see Figure S4), which has a smaller trend, similar to the 220 DU threshold, and is likely due to the later onset of

ozone depletion in that model. Interestingly, at 130 DU (Figure 3c), the WACCM6 ensemble shows very few years significantly exceeding this threshold after 2010. Between 2010 and 2019 only 80% of WACCM6 years reached the threshold, and between 2020 and 2024, only 60% of WACCM6 years did. For observations, only 2011, 2018, 2020, and 2021 noticeable surpass the threshold, but, still less than half of what was occurring during peak EESC loading (1999–2008).

The trends obtained in Figure 3 when only using a simple linear regression model, especially at 175 DU, show that during September the ozone hole is still displaying evidence of recovery despite 2015, 2018, 2020, and 2021 being outliers later in the season, in agreement with Figure 2.

In the case of October in Figure 4, the observations do not show a significant recovery trend for either the 220 or 175 DU thresholds at 0.31 ± 3.3 and -0.18 ± 3.5 million km^2/decade, respectively. There is a large amount of variability after 2000, with the 2015, 2020, and 2021 ozone holes as large, or in the case of 2015, larger than previous years of higher EESC loading. This is also seen in the WACCM6 ensemble (Figure 4a), which shows October trends for 220 DU of -2.4 ± 1.2 million km^2/decade compared to September of -3.4 ± 1.0 million km^2/decade. However, it is not captured in the WACCM4 ensemble (see Figure S5a), likely due to the delayed onset of ozone depletion (Figure 1). Much larger areas below 130 DU are also seen in both the model and observations as compared with September (Figure 3), with many more years reaching the threshold, especially in the observations; indeed, only 1998 and 2006 displayed larger observed areas compared to 2015, 2020, and 2021.

5. Conclusions

As the Antarctic ozone hole continues to recover, some large ozone holes have continued to occur. In this paper, we have analyzed key recovery metrics to investigate these recent large ozone hole years in the context of recovery.

We compared observations to a 10-member ensemble from the CESM1 WACCM4 model and a three-member ensemble from the CESM2 WACCM6 model for ozone hole areas in different years as a function of day of year, which revealed both the growth period in September and the shrinkage of the hole afterward. Based on these characteristics, we utilized three different ozone hole thresholds of 220, 175, and 130 DU and defined ozone hole start dates for these thresholds. Finally, time series of monthly ozone hole areas for the above thresholds were analyzed for September and October. The analysis illuminated three key metrics for Antarctic ozone recovery, and shows its robust continuation despite the occurrence of recent record-large ozone hole sizes (i.e., 2015, 2018, 2020, and 2021) at certain times of the year. These are:

1. Onset dates. The ozone hole start dates for three thresholds of 220, 175, and 130 DU are occurring later in the year over the recovery period of 2009–2018 in Figure 1; that is, the ozone hole is forming more slowly as EESC concentrations decrease, as expected. The recent extremely large ozone hole years of 2015, 2018, 2020, and 2021 also show a later ozone hole start date for all thresholds. This is also captured in the models for 175 and 130 DU, where it is shown that the 10 largest ensemble years for WACCM4 and 6 largest ensemble years for WACCM6 between 2015 and 2020 exhibit a clear later start date compared to 1999–2008. Ozone hole start date recovery trends over 2000–2021 are significant for both 220 and 175 DU, in good agreement with WACCM6. The later start dates for the rapid onset of ozone depletion is a robust sign of ozone recovery post-2000
2. Ozone hole size in September. Observed recovery trends over 2000–2021 in the size of the ozone hole during September are significant for the 220 and 175 DU thresholds. This is not captured in observed October trends, when the extreme ozone years of 2015, 2020, and 2021 are as large or larger compared to the 1999–2008. The September recovery trends are also noticeably larger than October in WACCM6
3. Ozone hole depth. Ozone holes that are deeper than the 130 DU threshold have become rarer after 2010 in both observations and WACCM6 in September, and this is a particularly robust sign of ozone recovery

As the simple regression model used here does not remove sources of variability such as the QBO, the trend values and significance should not be taken as an optimal estimate. However, a difference in the magnitude of the trends between September and October can be seen by inspection. Since both the ClO dimer and BrO-ClO catalytic cycles require ClO, the onset of ozone depletion is governed heavily by EESC concentration

after initial photolysis of Cl_2. Thus the onset of ozone recovery is a key time period to investigate, despite large ozone holes occurring later in the season, such as for 2015, 2018, 2020, and 2021. Indeed, the data suggests that while chemical processes dominate the early part of the ozone hole season from August through September, dynamical processes play a leading role in determining ozone hole size and depth later, that is, October through December.

Finally, this work indicates that even though large ozone holes will likely continue to occur in the future, either through dynamical variability alone, or exacerbated by large volcanic eruptions or major fire smoke inputs to the stratosphere, the recovery of the ozone hole is still occurring and will be able to be identified by focusing on the three metrics identified here.

Data Availability Statement

BS-TCO data can be obtained at: https://doi.org/10.5281/zenodo.4535247. OMI data can be found at: https://earthdata.nasa.gov/earth-observation-data/near-real-time/download-nrt-data/omi-nrt. WACCM4 data used in this paper are freely available at: http://doi.org/10.7910/DVN/V5R9WV. WACCM6 data used in this paper are available at: https://esgf-node.llnl.gov/search/cmip6/.

Acknowledgments
K. A. Stone and S. Solomon were supported by a gift to MIT from an anonymous donor and by a grant from the National Science Foundation NSF 1848863. D. E. Kinnison was funded in part by NASA grant (80NSSC19K0952). Cheyenne: HPE/SGI ICE XA System (NCAR Community Computing). Boulder, CO: National Center for Atmospheric Research. doi:10.5065/D6RX99HX. The authors would like to thank Bodeker Scientific for providing the BS-filled total column ozone database.

References

Bodeker, G. E., & Kremser, S. (2021). Indicators of Antarctic ozone depletion. *Atmospheric Chemistry and Physics*, *21*, 5289–5300. https://doi.org/10.5194/acp-21-5289-2021

Bodeker, G. E., Kremser, S., & Tradowsky, J. S. (2021). *BS filled total column database V3.5.1 (Version 3.5.1)*. Zenodo. https://doi.org/10.5281/zenodo.3908786

Bodeker, G. E., Nitzbon, J., Tradowsky, J. S., Kremser, S., Schwertheim, A., & Lewis, J. (2021). A global total column ozone climate data record. *Earth System Science Data*, *13*(8), 3885–3906. https://doi.org/10.5194/essd-13-3885-2021

Chipperfield, M. P., Bekki, S., Dhomse, S., Harris, N. R. P., Hassler, B., Hossaini, R., et al. (2017). Detecting recovery of the stratospheric ozone layer. *Nature*, *549*, 211–218. https://doi.org/10.1038/nature23681

Dhomse, S. S., Kinnison, D., Chipperfield, M. P., Salawitch, R. J., Cionni, I., Hegglin, M. I., et al. (2018). Estimates of ozone return dates from Chemistry-Climate Model Initiative simulations. *Atmospheric Chemistry and Physics*, *18*(11), 8409–8438. https://doi.org/10.5194/acp-18-8409-2018

Engel, A., Bönisch, H., Ostermöller, J., Chipperfield, M. P., Dhomse, S., & Jöckel, P. (2018). A refined method for calculating equivalent effective stratospheric chlorine. *Atmospheric Chemistry and Physics*, *18*(2), 601–619. https://doi.org/10.5194/acp-18-601-2018

Garcia, R. R., Smith, A. K., Kinnison, D. E., de la Cámara, Á., & Murphy, D. J. (2017). Modification of the gravity wave parameterization in the Whole Atmosphere Community Climate Model: Motivation and results. *Journal of the Atmospheric Sciences*, *74*(1), 275–291. https://doi.org/10.1175/JAS-D-16-0104.1

Gettelman, A., Mills, M. J., Kinnison, D. E., Garcia, R. R., Smith, A. K., Marsh, D. R., et al. (2019). The Whole Atmosphere Community Climate Model Version 6 (WACCM6). *Journal of Geophysical Research: Atmospheres*, *124*(23), 12380–12403. https://doi.org/10.1029/2019JD030943

Hassler, B., Daniel, J. S., Johnson, B. J., Solomon, S., & Oltmans, S. J. (2011). An assessment of changing ozone loss rates at South Pole: Twenty-five years of ozonesonde measurements. *Journal of Geophysical Research*, *116*(22). https://doi.org/10.1029/2011JD016353

Ivy, D. J., Solomon, S., Kinnison, D., Mills, M. J., Schmidt, A., & Neely, R. R. (2017). The influence of the Calbuco eruption on the 2015 Antarctic ozone hole in a fully coupled chemistry-climate model. *Geophysical Research Letters*, *44*, 1–2561. https://doi.org/10.1002/2016GL071925

Ivy, D. J., Solomon, S., & Rieder, H. E. (2016). Radiative and dynamical influences on polar stratospheric temperature trends. *Journal of Climate*, *29*(13), 4927–4938. https://doi.org/10.1175/JCLI-D-15-0503.1

Kinnison, D. E., Brasseur, G. P., Walters, S., Garcia, R. R., Marsh, D. R., Sassi, F., et al. (2007). Sensitivity of chemical tracers to meteorological parameters in the MOZART-3 chemical transport model. *Journal of Geophysical Research*, *112*, D20302. https://doi.org/10.1029/2006JD007879

Kramarova, N. A., Newman, P. A., Nash, E. R., Strahan, S. E., Long, C. S., Johnson, B., et al. (2019). Antarctic ozone hole [in "State of the CLimate in 2019"]. *Bulletin of the American Meteorological Society*, *101*(8), S310–S312. https://doi.org/10.1175/BAMS-D-20-0090.1

Kuttippurath, J., Kumar, P., Nair, P. J., & Pandey, P. C. (2018). Emergence of ozone recovery evidenced by reduction in the occurrence of Antarctic ozone loss saturation. *npj Climate and Atmospheric Science*, *1*(42). https://doi.org/10.1038/s41612-018-0052-6

Levelt, P. F., Hilsenrath, E., Leppelmeier, G. W., van den Oord, G. H. J., Bhartia, P. K., Tamminen, J., et al. (2006). Science objectives of the ozone monitoring instrument. *IEEE Transactions on Geoscience and Remote Sensing*, *44*(5), 1199–1208. https://doi.org/10.1109/TGRS.2006.872336

Lickley, M., Solomon, S., Fletcher, S., Velders, G. J. M., Daniel, J., Rigby, M., et al. (2020). Quantifying contributions of chlorofluorocarbon banks to emissions and impacts on the ozone layer and climate. *Nature Communications*, *11*(1). https://doi.org/10.1038/s41467-020-15162-7

Meinshausen, M., Nicholls, Z. R. J., Lewis, J., Gidden, M. J., Vogel, E., Freund, M., et al. (2020). The shared socio-economic pathway (SSP) greenhouse gas concentrations and their extensions to 2500. *Geoscientific Model Development*, *13*(8), 3571–3605. https://doi.org/10.5194/gmd-13-3571-2020

Mills, M. J., Schmidt, A., Easter, R., Solomon, S., Kinnison, D. E., Ghan, S. J., et al. (2016). Global volcanic aerosol properties derived from emissions, 1990-2014, using CESM1(WACCM). *Journal of Geophysical Research: Atmospheres*, *121*, 2332–2348. https://doi.org/10.1002/2015JD024290

Molina, M. J., Tso, T. L., Molina, L. T., & Wang, F. C. Y. (1987). Antarctic stratospheric chemistry of chlorine nitrate, hydrogen chloride, and ice: Release of active chlorine. *Science*, *238*(4831), 1253–1257. https://doi.org/10.1126/science.238.4831.1253

Montzka, S. A., Dutton, G. S., Yu, P., Ray, E., Portmann, R. W., Daniel, J. S., et al. (2018). An unexpected and persistent increase in global emissions of ozone-depleting CFC-11. *Nature*, *557*(7705), 413–417. https://doi.org/10.1038/s41586-018-0106-2

Neely, R. R. I., & Schmidt, A. (2016). *VolcanEESM: Global volcanic sulphur dioxide (SO_2) emissions database from 1850 to present—version 1.0*. Centre for Environmental Data Analysis. https://doi.org/10.5285/76ebdc0b-0eed-4f70-b89e-55e606bcd568

Newman, P. A., Daniel, J. S., Waugh, D. W., & Nash, E. R. (2007). A new formulation of equivalent effective stratospheric chlorine (EESC). *Atmospheric Chemistry and Physics*, *7*(17), 4537–4552. https://doi.org/10.5194/acp-7-4537-2007

Pazmiño, A., Godin-Beekmann, S., Hauchecorne, A., Claud, C., Khaykin, S., Goutail, F., et al. (2018). Multiple symptoms of total ozone recovery inside the Antarctic vortex during austral spring. *Atmospheric Chemistry and Physics*, *18*(10), 7557–7572. https://doi.org/10.5194/acp-18-7557-2018

Solomon, S. (1999). Stratospheric ozone depletion: A review of concepts and history. *Reviews of Geophysics*, *37*(3), 275–316. https://doi.org/10.1029/1999RG900008

Solomon, S., Ivy, D. J., Kinnison, D., Mills, M. J., Neely, R. R., & Schmidt, A. (2016). Emergence of healing in the Antarctic ozone layer. *Science*, *310*, 307–274. https://doi.org/10.1126/science.aae0061

Stone, K. A., Solomon, S., & Kinnison, D. E. (2018). On the identification of ozone recovery. *Geophysical Research Letters*, *45*, 5158–5165. https://doi.org/10.1029/2018GL077955

Stone, K. A., Solomon, S., Kinnison, D. E., Baggett, C. F., & Barnes, E. A. (2019). Prediction of Northern Hemisphere regional surface temperatures using stratospheric ozone information. *Journal of Geophysical Research: Atmospheres*, *124*, 5922–5933. https://doi.org/10.1029/2018JD029626

Stone, K. A., Solomon, S., Kinnison, D. E., Pitts, M. C., Poole, L. R., Mills, M. J., et al. (2017). Observing the impact of Calbuco volcanic aerosols on south polar ozone depletion in 2015. *Journal of Geophysical Research: Atmospheres*, *122*(21), 11–862. https://doi.org/10.1002/2017JD026987

Strahan, S. E., Douglass, A. R., & Damon, M. R. (2019). Why do Antarctic ozone recovery trends vary? *Journal of Geophysical Research: Atmospheres*, *124*(15), 8837–8850. https://doi.org/10.1029/2019JD030996

Strahan, S. E., Douglass, A. R., Newman, P. A., & Steenrod, S. D. (2014). Inorganic chlorine variability in the Antarctic vortex and implications for ozone recovery. *Journal of Geophysical Research: Atmospheres*, *119*, 14098–14109. https://doi.org/10.1002/2014jd022295

Weatherhead, E. C., Reinsel, G. C., Tiao, G. C., Jackman, C. H., Bishop, L., Hollandsworth Frith, S. M., et al. (2000). Detecting the recovery of total column ozone. *Journal of Geophysical Research*, *105*(D17), 22201–22210. https://doi.org/10.1029/2000JD900063

WMO, World Meteorological Organization. (2018). *Scientific assessment of ozone depletion: 2018. Global ozone research and monitoring project, report no. 58* (p. 588).

Yamazaki, Y., Matthias, V., Miyoshi, Y., Stolle, C., Siddiqui, T., Kervalishvili, G., et al. (2020). September 2019 Antarctic sudden stratospheric warming: Quasi-6-day wave burst and ionospheric effects. *Geophysical Research Letters*, *47*(1), 1–12. https://doi.org/10.1029/2019GL086577

Yu, P., Davis, S. M., Toon, O. B., Portmann, R. W., Bardeen, C. G., Barnes, J. E., et al. (2021). Persistent stratospheric warming due to 2019–2020 Australian wildfire smoke. *Geophysical Research Letters*, *48*(7), e2021GL092609. https://doi.org/10.1029/2021gl092609

Zhu, Y., Toon, O. B., Kinnison, D., Harvey, V. L., Mills, M. J., Bardeen, C. G., et al. (2018). Stratospheric aerosols, polar stratospheric clouds and polar ozone depletion after the Mt. Calbuco eruption in 2015. *Journal of Geophysical Research: Atmospheres*, *123*, 12–308. https://doi.org/10.1029/2018JD028974